Lidar observations of interacting wind turbine wakes in an onshore wind farm

Julie K. Lundquist [1,2], Eugene S. Takle [3], Matthieu Boquet [4], Branko Kosović [5], Michael E. Rhodes[1], Daniel Rajewski[3], Russell Doorenbos [3], Samantha Irvin [3], Matthew L. Aitken[1], Katja Friedrich[1], Paul T. Quelet[1], Jiwan Rana[1], Clara St. Martin[1], Brian Vanderwende, [1]Rochelle Worsnop[1]

[1] University of Colorado at Boulder
[2] National Renewable Energy Laboratory
[3] Iowa State University
[4] Leosphere
[5] National Center for Atmospheric Research

Corresponding Author: Julie.Lundquist@colorado.edu, voice:+001 303/492-8932

Abstract

Detailed observations of the interactions of wakes of multiple turbines in large onshore wind farms are required for validation of detailed flow simulation models for assessing and forecasting wind power production and loads on individual turbines. The CWEX-13 field campaign was designed to explore the propagation of individual turbine wakes as well as the interaction of multiple wakes in a range of atmospheric stability conditions. CWEX-13 took place between late June and early September 2013 in a 150 MW wind farm in central Iowa, the same wind farm studied in previous CWEX campaigns. The region is characterized by flat topography and enjoys strong diurnal cycles of atmospheric stability as well as regular occurrences of nocturnal low-level jets. Multiple remote sensing systems characterized winds, temperature, and moisture profiles throughout the wind farm, complementing the array of surface-based meteorological stations.

Keyword

remote sensing, lidar, turbine wakes, wake interactions, atmospheric stability

1 Introduction

As wind energy deployment grows, questions arise regarding how wind plants affect the local environment. The 2010 and 2011 field campaigns of the Crop-Wind Energy Experiment (CWEX) [1-3] quantified the effects of one row of turbines on the local environment. In the 2013 CWEX field campaign presented here, multiple remote sensing instruments quantified the spatial variability of winds and turbulence through the complex flow of multiple rows of a ~ 150 MW onshore wind plant. The science goals of the CWEX-13 campaign include:

- Document the effect of atmospheric stability on characteristics of wind turbine wakes (wind speed deficit, wake expansion, wake meandering) after one row and after multiple rows;
- Quantify the impact of atmospheric stability, wind shear, and wind veer on wind plant power production;
- Collect detailed wind and turbulence data to evaluate and improve wind plant parameterizations in numerical weather prediction and large-eddy simulation models, with attention to development of convergence zones within wind plants, speed-up areas beneath and between turbines, surface fluxes of heat/momentum/moisture, and turbulence dissipation within wakes after a single row, double row, and multiple rows of turbines;
- Document the variability of the nocturnal low-level jet (LLJ) upwind and within a wind farm.

2 Experimental Design

The previous CWEX experiments utilized profiling lidar systems (Leosphere/Renewable NRG Systems WINDCUBE™ v1 systems) to quantify wake wind speed deficits and wake turbulence enhancements in the near-wake region. In CWEX-11, one lidar was located ~ 2 rotor diameters D south (typically upwind) of one row of turbines to quantify inflow conditions. Another lidar located ~ 3D north (typically downwind) provided quantification of the wake impacts during southerly flow conditions. Wake wind speed deficits were largest during wind speeds just slower than rated speed, when the turbine thrust coefficient was at maximum value [2]. Analysis of surface flux measurements suggests that turbines significantly enhance nocturnal surface carbon dioxide and sensible heat fluxes downwind [3].

The CWEX-13 field campaign expanded these observations to consider far-wake impacts and the impacts of multiple rows of turbines. The field campaign took place between late June and early September 2013 in a 150 MW wind farm in central Iowa, the same wind farm studied in the previous CWEX campaigns. The wind plant is laid roughly as a parallelogram with major axis extending from the northwest to the southeast and sides approximately 10 km x 25 km. Land use in the wind plant is almost entirely devoted to large fields of corn (height 1-2 m) and soybeans (height 0.3-0.8 m) except for four small villages, occasional riparian regions, and widely scattered farmsteads with a few trees and buildings.

In the region of interest in CWEX-13, turbines of nominally 80m hub height and 80 m rotor diameter D were located in rows separated by 20 D. Three WINDCUBE™ v1 profiling lidar systems (provided by the University of Colorado at Boulder and the National Center for Atmospheric Research) were located a) south of the first turbine row, b) 8.5D north of the first turbine row, and c) 5.7 D north of a second row of turbines (Figure 1). These instruments provide profiles of wind speed and direction from 40 m to 220 m above the surface and have successfully characterized inhomogeneous flow such as wind turbine wakes with quantifiable error [2], although the standard deviations of velocities as measured by such lidars are not the same as turbulence metrics measured by sonic anemometer or other in situ instrumentation [4].

Complementary instrumentation included a Radiometrics MP-3000A microwave radiometer (University of Colorado at Boulder) to quantify atmospheric stability [5] and several surface flux stations (Iowa State University). Finally, for a portion of the CWEX-13 campaign (31 July – 6 September), a WINDCUBE™ 200S from LEOSPHERE was co-located with the northernmost WINDCUBE™ v1 lidar to enable instrument intercomparisons as well as horizontal scans of the turbine wakes and vertical scans of the wake from one individual turbine.

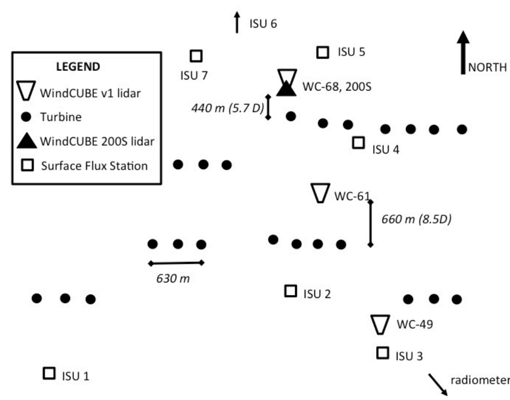

Figure 1: Schematic diagram of the CWEX-13 instrument deployment

3 Lidar Performance

Profiling lidars operated throughout the CWEX-13 observing period, while a scanning lidar operated for a portion of the observational campaign.

WC-49 (collocated with surface flux station ISU3) provided freestream or upwind measurements during southerly flow conditions. As seen in Figure 1, WC-61 collected wind profiles 8.5*D* north of the “first” row of turbines, sampling the far-wake region. A second row of turbines (approximately 20 *D* downwind of the first row) is followed by a third lidar (WC-68) located 5.7*D* north of the closest turbine. These three lidars were deployed on 27 June 2013 and removed from the field on 5 September 2013. Before the deployment, the three lidars were operated next to each other for a short time period to ensure calibration (Figure 2), as in [2]. The agreement between the instruments is excellent: after the lidars were moved to different locations, the differences observed in the wind field may be attributed to the wind field and not to variations between the instruments.

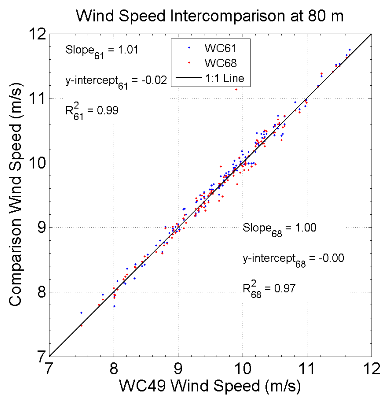

Figure 2: Intercomparison of three collocated WindCUBE v1 lidars from the afternoon of 28 June 2013 based on 2-minute averages of horizontal wind speed; all three lidars were located at site A3 during this time period. Data from WC68 (red) and WC61 (blue) are compared to data from WC49.

Over the course of the field campaign, data retrieval was near 100 percent at all levels below 120 m, with the poorest performance (96% data available within the turbine rotor disk altitudes) at location A2 due primarily to a power failure.

The scanning strategy for the WINDCUBE™ 200S (which was co-located with one WINDCUBE™ v1 lidar) was based on a 30-minute cycle. For three minutes, a 60-degree elevation, 360-degree azimuthal PPI scan was conducted, followed by a 75-degree elevation, 360-degree azimuthal PPI scan. These scans were intended for comparison with the collocated WINDCUBE™ v1 observations to “calibrate” the WINDCUBE™ 200S measurements. Initial comparisons of the horizontal winds retrieved with the two systems show excellent agreement (Figure 3) despite slight differences in the measurement elevations and averaging times (3-minutes for the 200S and 2-minutes for the v1).

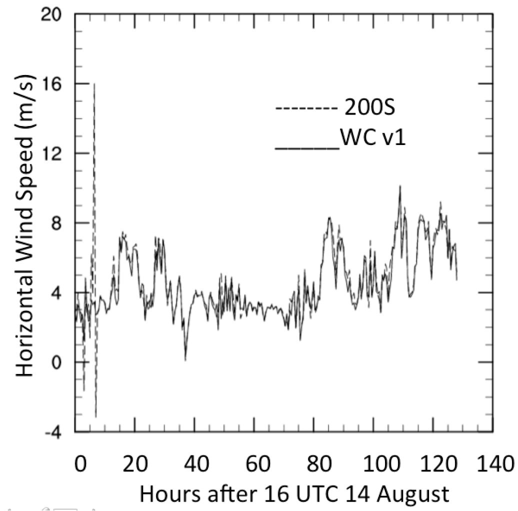

Figure 3: Comparison of 200S retrievals of horizontal wind speed from 60-degree elevation, 360-degree azimuthal scan from the first range gate (86m above ground), as compared to 80-meter altitude measurements from WC v1. The large excursions in the first several hours occur during times of low carrier-to-noise ratio.

4 Meteorological Variability

The experimental design of CWEX-13 relied upon frequent southeasterly-southwesterly winds to enable “upwind” and “downwind” measurements around the two rows of turbines of focus. Climatology for this region [1] supports such a field design. Wind roses (Figure 4) from the 40m, 120m, and 220m altitudes from the southernmost (undisturbed) lidar show that wind conditions were predominantly southeasterly-southwesterly, with infrequent northerly and northwesterly wind cases. These northerly flow cases were typically associated with frontal passages. The wind roses suggest slight veering of the wind direction with height, likely due to nocturnal veering during stable conditions associated with the nocturnal low-level jet [6-8]. Analysis is underway to quantify if this veering is indeed most strongly associated with strong stability conditions or if there is a large-scale mesoscale veering due to the enhanced roughness of the wind farm.

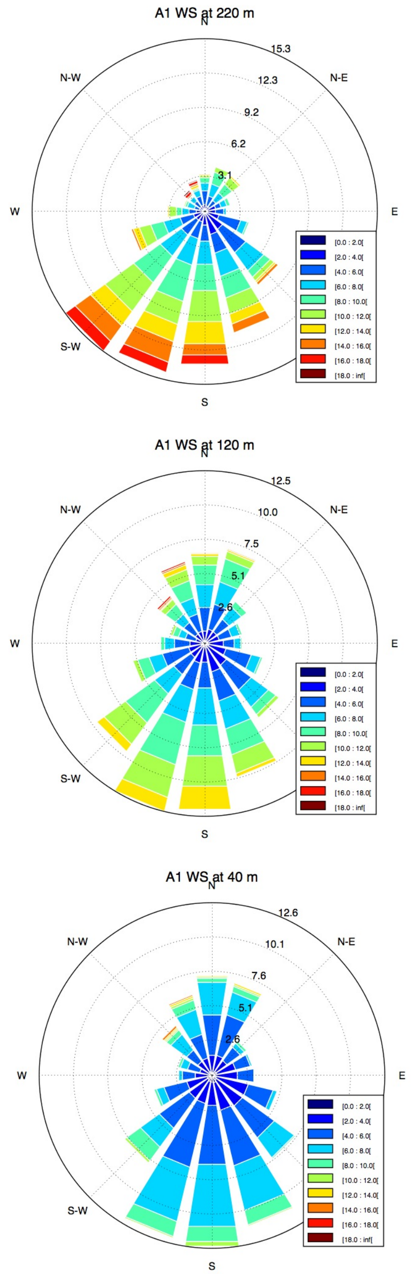

Figure 4: Wind roses for all times of day at 220-m (top), 120-m (center), and 40-m (bottom) above the surface from the southern WINDCUBE™ location. The veering with height (change of direction from southerly at 40-m to southwesterly at 220-m) tends to occur at night.

The frequent southerly conditions enabled the WINDCUBE™ 200S from LEOSPHERE, when operating in plan-position-indicator ("horizontal slice") mode, to observe multiple wakes propagating from either row of turbines depending on the scanning elevation of the lidar, similar to the study of [9, 10]. Because the 200S lidar was located on the ground, the horizontal scans were taken at a range of elevation angles, documenting velocities at different altitudes depending on the distance from the lidar. Figure 5 shows an example of these wakes as observed with a scan from ~ 2 UTC under southwesterly flow conditions (darker blue represents faster flow towards the lidar). The scan of 50 degrees in azimuth at a scanning rate of 0.5 degrees per second required 100 seconds of scan time. The elevation angle of this scan collects data at an elevation of approximately 110m at the row of turbines visualized here, the southerly row of turbines. (At this elevation angle, at the range of the northerly row of turbines, the lidar scan is at 20 m above the surface, underneath that row of turbines, so the northernmost row of turbines is not visible in this scan.) The degradation or "recovery" of the wake with downwind distance is clearly visible, but quantification of wake expansion rates requires quantitative analysis that considers the change of altitude with range. The quantitative approach of [10], previously applied to scanning lidar measurements of wakes from a single turbine, will be applied to these data. Goals include measuring interactions between turbine wakes, quantifying variation of wake characteristics with atmospheric stability, and quantifying wake meandering.

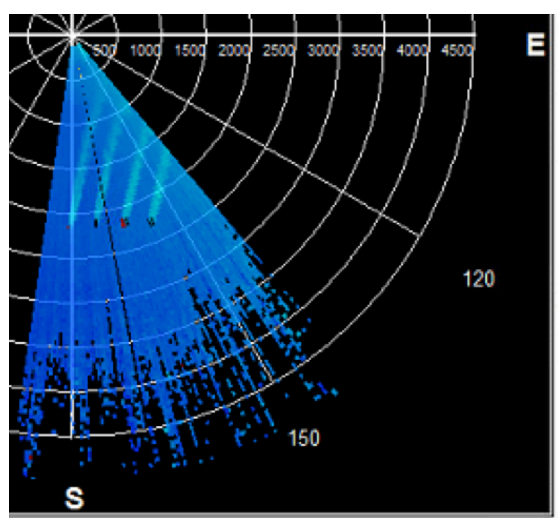

Figure 5: Example PPI scan showing turbine wakes propagating to the northeast from the row of turbines approximately 2000m from the WINDCUBE™ 200S scanning lidar.

Many of the science goals of CWEX-13 focus on the effect of atmospheric stability on turbine wake evolution. As a result, the field program design incorporated multiple measurements for quantifying atmospheric stability. The primary means for quantifying atmospheric stability is via measurement of the Obukhov length from sonic anemometers mounted on 10 m surface flux stations. In addition to these measurements, this campaign involved the use of a microwave radiometer (Radiometrics MP-3000A) to quantify the vertical variation of temperature and moisture. The Brunt-Vaisala frequency can be calculated from such temperature profile data [5], and will be compared to Obukhov lengths estimated by surface-based sonic anemometer data.

Example time-height cross-sections of temperature and moisture exhibit the strong diurnal cycle characteristic of the summertime Midwestern United States (Figure 6). Surface-driven cooling over the night (0000-1200 UTC) is evident, as well as strong heating of the surface during the day. During this 24-hour period, winds are consistently southerly or southwesterly (Figure 7, bottom panel). During the night, a nocturnal low-level jet developed, with maximum observed wind speeds of 17 m s^{-1} just 200 m above the surface. Analysis of the 200S WINDCUBE™ data (not shown) suggests that this jet extends through a depth of several hundred meters.

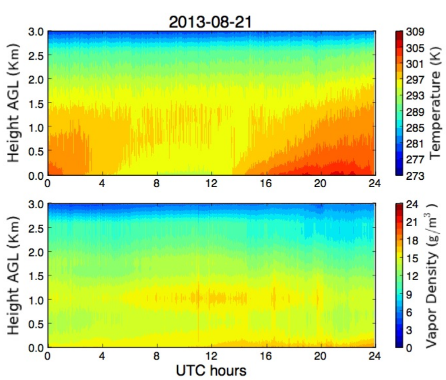

Figure 6: Time-height cross section of temperature (top) and water vapor density (bottom) from the radiometer for the 24-hr period starting at 00 UTC on 21 August 2013.

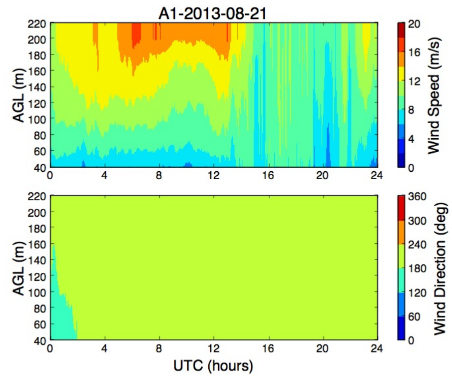

Figure 7: Time-height cross-section of wind speed (top) and wind direction (bottom) from the southernmost lidar for the 24-hr period starting at 00 UTC on 21 August 2013.

5 Conclusion

The CWEX-13 field campaign employed a suite of remote sensing and in situ instruments to explore the dynamics and thermodynamics of the complex wind flow through multiple rows of a ~ 150 MW onshore wind plant in the Midwestern United States. Turbines of nominally 80-m hub height and 80-m rotor diameter D were located in rows separated by 20D in the area of observation in CWEX-13. WINDCUBE™ v1 lidar wind profiles at three locations within the wind plant (upwind, 8.5D past a first row, and 5.7D past a second row) provided observation of wind speed deficits and turbulence enhancements within the turbine wakes during southerly flow conditions. Scanning lidar (WINDCUBE™ 200S from LEOSPHERE) measurements of line-of-sight velocity enabled assessments of wake locations for comparison with the profiling lidar measurements, as well as data for quantification of wake characteristics. Retrievals of temperature and moisture profiles from a microwave radiometer (Radiometrics MP-3000A) quantify atmospheric stability via the Brunt-Vaisala frequency. Finally, surface flux stations equipped with sonic anemometers at several locations within the wind plant document atmospheric stability as well as surface fluxes of heat, momentum, and moisture to identify the impact of multiple rows of turbines on surface-atmosphere exchange processes.

Initial analysis from CWEX-13 suggest that the dataset includes numerous observations of nocturnal low-level jets interacting with the wind farm. Furthermore, these data may be used to validate wind plant representations in numerical weather prediction models, such as the Weather Research and Forecasting (WRF) wind farm parameterization [11,12]. The detailed observations of multiple wakes from two rows of turbines may prove useful for comparison to more explicit turbine-resolving models such as available in OpenFOAM [13], the Large-Eddy Simulation capability of WRF [14], and others [15]; WindBlade: http://ees.lanl.gov/ees16/windblade.shtml). Evaluation of the turbine power data in conjunction with these meteorological data, as in [16] and [17], will enable insight into the impacts of atmospheric stability on power performance in this region [18,19].

References:

[1] Rajewski, D., G. Takle, J. K. Lundquist, M. E. Rhodes, S. Oncley, T. Horst. 2013a. Crop Wind Energy Experiment (CWEX): Observations of Surface-Layer, Boundary Layer, and Mesoscale Interactions with a Wind Farm. *Bull Amer Meteor Soc* 94: 655–672.

[2] Rhodes, M. E., and J. K. Lundquist. 2013. The Effect of Wind Turbine Wakes on Summertime Midwest Atmospheric Wind Profiles. *Boundary-Layer Meteorology* 149, 85-103. doi:10.1007/s10546-013-9834-x

[3] Rajewski, D., E. S. Takle, J. K. Lundquist, J. H. Prueger, R. Pfeiffer, J. L. Hatfield, K. K. Spoth, and R. K. Doorenbos. 2014. Changes in fluxes of heat, H2O, and CO2 caused by a large wind farm. In review at *Agricultural & Forest Meteorology.*

[4] Sathe, A., J. Mann, J. Gottschall, and M. S. Courtney. 2011. Can Wind Lidars Measure Turbulence? *J Atmos and Oceanic Technol* 28: 853–868.

[5] Friedrich, K. J. K. Lundquist, E. Kalina, M. Aitken, and R. Marshall. 2012. Stability and Turbulence in the Atmospheric Boundary Layer: An Intercomparison of Remote Sensing and Tower Observations. *Geophys. Res. Lett.*, Vol. 39, No. 3, L03801, doi:10.1029/2011GL050413.

[6] Blackadar, A. K. 1957. Boundary-Layer Wind Maxima and their Significance for the Growth of Nocturnal Inversions. Bulletin of the American Meteorological Society, 38, 283-290.

[7] Banta, R. M., R. K. Newsom, J. K. Lundquist, Y. L. Pichugina, R. L. Coulter, and L. Mahrt. 2002. Nocturnal low-level jet characteristics over Kansas during CASES-99. Boundary-Layer Meteorology 105 (2), 221-252.

[8] Kelley, N.D., B. J. Jonkman, and G. N. Scott. 2006. The Great Plains Turbulence Environment: Its Origins, Impact and Simulation. AWEA's 2006 WindPower Conference Pittsburgh, Pennsylvania June 4–7, 2006. Available at http://www.nrel.gov/docs/fy07osti/40176.pdf

[9] Smalikho, I. N., V. A. Banakh, Y. L. Pichugina, W. A. Brewer, R. M. Banta, J. K. Lundquist, and N. D. Kelley. 2013. Lidar investigation of atmosphere effect on a wind turbine wake. In press at *J. Atmos. Ocean. Tech.* http://dx.doi.org/10.1175/JTECH-D-12-00108.1

[10] Aitken, M. L., J. K. Lundquist, Y. L. Pichugina, and R. M. Banta. 2014. Quantifying wind turbine wake characteristics from scanning remote sensor data. *J. Atmos. Ocean. Tech.* 10.1175/JTECH-D-13-00104.1

[11] Fitch, A. C., J. B. Olson, J. K. Lundquist, J. Dudhia, A. K. Gupta, J. Michalakes, and I. Barstad. 2012. Local and Mesoscale Impacts of Wind Farms as Parameterized in a Mesoscale NWP Model. *Monthly Weather Review.* Vol. 140, No. 9, 3017-3038.

http://dx.doi.org/10.1175/MWR-D-11-00352.1

[12] Fitch, A., J. K. Lundquist, and J. B. Olson. 2013. Mesoscale Influences of Wind Farms throughout a diurnal cycle. *Monthly Weather Review*, 141, 2173-2198. doi: http://dx.doi.org/10.1175/MWR-D-12-00185.1

[13] Churchfield, M. J., S. Lee, J. Michalakes, P. J. Moriarty. 2012. A numerical study of the effects of atmospheric and wake turbulence on wind turbine dynamics. *J Turbulence* 13: 1-32

[14] Mirocha, J., B. Kosovic, M. Aitken, and J. K. Lundquist. 2014. Implementation of a generalized actuator disk wind turbine model into WRF for large-eddy simulation applications. J. Renewable Sustainable Energy **6,** 013104 (2014); http://dx.doi.org/10.1063/1.4861061

[15] Lu, H. and F. Porte-Agel. 2011. Large-eddy simulation of a very large wind farm in a stable atmospheric boundary layer. Phys. Fluids, 23, 065 101, doi:10.1063/1.3589857.

[16] Barthelmie, R.J., Pryor, S.C., Frandsen, S.T., Hansen, K.S., Schepers, J.G., Rados, K., Schlez, W., Neubert, A., Jensen, L.E. and Neckelmann, S. 2009. Quantifying the impact of wind turbine wakes on power output at offshore wind farms. Journal of Atmospheric and Oceanic Technology, 27, 1302–1317. doi: 10.1175/2010JTECHA1398.1

[17] Hansen, K. S., R. J. Barthelmie, L. E. Jensen, and A. Sommer. 2012. The impact of turbulence intensity and atmospheric stability on power deficits due to wind turbine wakes at Horns Rev wind farm. Wind Energy, 15, 183-196.

[18] Vanderwende, B. and J. K. Lundquist. 2012. The modification of wind turbine performance by statistically distinct atmospheric regimes. *Environmental Research Letters* 7 (2012) 034035 doi:10.1088/1748-9326/7/3/034035

[19] Wharton, S. and J. K. Lundquist. 2012. Atmospheric Stability Affects Wind Turbine Power Collection. *Environ. Res. Lett.* 7 014005 doi:10.1088/1748-9326/7/1/014005